ACS APPLIED MATERIALS & INTERFACES

Research Article

www.acsami.org

Carbon-Nanohorn-Reinforced Polymer Matrix Composites: Synergetic Benefits in Mechanical Properties

Sourabh B. Kadambi,[†,§] K. Pramoda,[‡,§] U. Ramamurty,[*,†,‡] and C. N. R. Rao[‡]

[†]Department of Materials Engineering, Indian Institute of Science, Bangalore-560012, India

[‡]International Centre for Materials Science, and New Chemistry Unit, Jawaharlal Nehru Centre for Advanced Scientific Research, Jakkur, Bangalore 560064, India

Supporting Information

ABSTRACT: Mechanical properties of single-walled carbon nanohorns (SWNH) and SWNH plus few-layer graphene (EG)-reinforced poly(vinyl alcohol) (PVA) matrix composites have been measured using the nanoindentation technique. The elastic modulus (E) and hardness (H) of PVA were found to improve by ∼315% and ∼135%, respectively, upon the addition of just 0.4 wt % SWNH. These properties were found to be comparable to those obtained upon the addition of 0.2 wt % single-walled nanotubes (SWNT) to PVA. Furthermore, upon binary addition of 0.2 wt % EG and 0.4 wt % SWNH to PVA, benefits in the form of ∼400% and ∼330% synergy in E and H, respectively, were observed, along with an increased resistance to viscoelastic deformation. The reasons for these improvements are discussed in terms of the dimensionality of nanocarbon, the effectiveness of nanocarbon and polymer matrix interaction, and the influence of nanocarbon on the degree of crystallinity of the polymer. The results from SWNH reinforcement in this study demonstrate the scope for a novel and, in contrast to SWNT composites, a commercially feasible opportunity for strengthening polymer matrices.

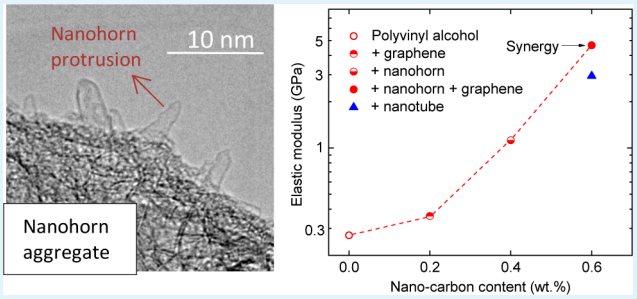

KEYWORDS: *carbon nanohorn, polymer nanocomposites, nanoindentation, mechanical properties, synergy*

1. INTRODUCTION

Nanocarbons such as nanotubes, graphene, and nanodiamond have shown great potential as fillers for strengthening polymer matrices.[1−3] Among them, single-walled nanotubes (SWNTs) in particular have demonstrated extraordinary strengthening ability.[4−6] Despite the immense potential, SWNTs are yet to find use in large-scale applications, because of high cost and limited availability.[5,7] For instance, the formation of metallic and carbonaceous impurities during SWNT synthesis leads to the requirement for extensive post-production purification processes.[8] These drawbacks prompt us to turn our attention toward another nanocarbon, viz. single-walled nanohorns (SWNHs), since they can be produced with excellent purity (92%−95%)[9] without the need for additional purification, and thus promise to be commercially viable.

SWNHs are tubular structures similar to SWNTs with a horn-shaped tip at one of their ends.[10] Similar to SWNTs, which aggregate into cylindrical bundles, SWNHs aggregate in the form of spherically shaped entities with outward protrusions of individual nanohorns from the surface of the aggregate.[10,11] Unlike SWNT bundles, which can be dispersed into individual, one-dimensional nanotubes, SWNH aggregates cannot be separated into individual species by chemical functionalization.[12] While the one-dimensionality and the high aspect ratio of a well-dispersed SWNT reinforcement provides the benefits of enhanced mechanical properties in polymer composites, the influence of the three-dimensionality of SWNH aggregate, together with the one-dimensionality of the individual protrusions of SWNH aggregates on the mechanical properties of polymers, has not been explored. Thus, in the current study, we investigate the ability of the SWNH aggregates to strengthen a semicrystalline polymer, poly(vinyl alcohol) (PVA). The nanoindentation technique is used for this purpose to study the elastic, plastic, and time-dependent responses of the composite. Also, in order to place the properties of SWNH−PVA composites in perspective, we estimate the properties of SWNT−PVA and few-layer graphene EG−PVA composites, both of which were prepared and tested under conditions similar to those of SWNH−PVA.

The selection of PVA as the matrix material in the present study is due to its water solubility, which aids the uniform dispersion of nanocarbons in the composite. For SWNHs, the use of PVA and chemical functionalization helps to disperse SWNH aggregates from grouped clusters or agglomerates. The estimation of the mechanical properties of PVA with a well-dispersed SWNH aggregate as reinforcement thus aims to provide an assessment of the potential of SWNH aggregates to strengthen polymers of importance to engineering and

Received: March 31, 2015
Accepted: July 17, 2015
Published: July 17, 2015

DOI: 10.1021/acsami.5b02792
ACS Appl. Mater. Interfaces 2015, 7, 17016−17022

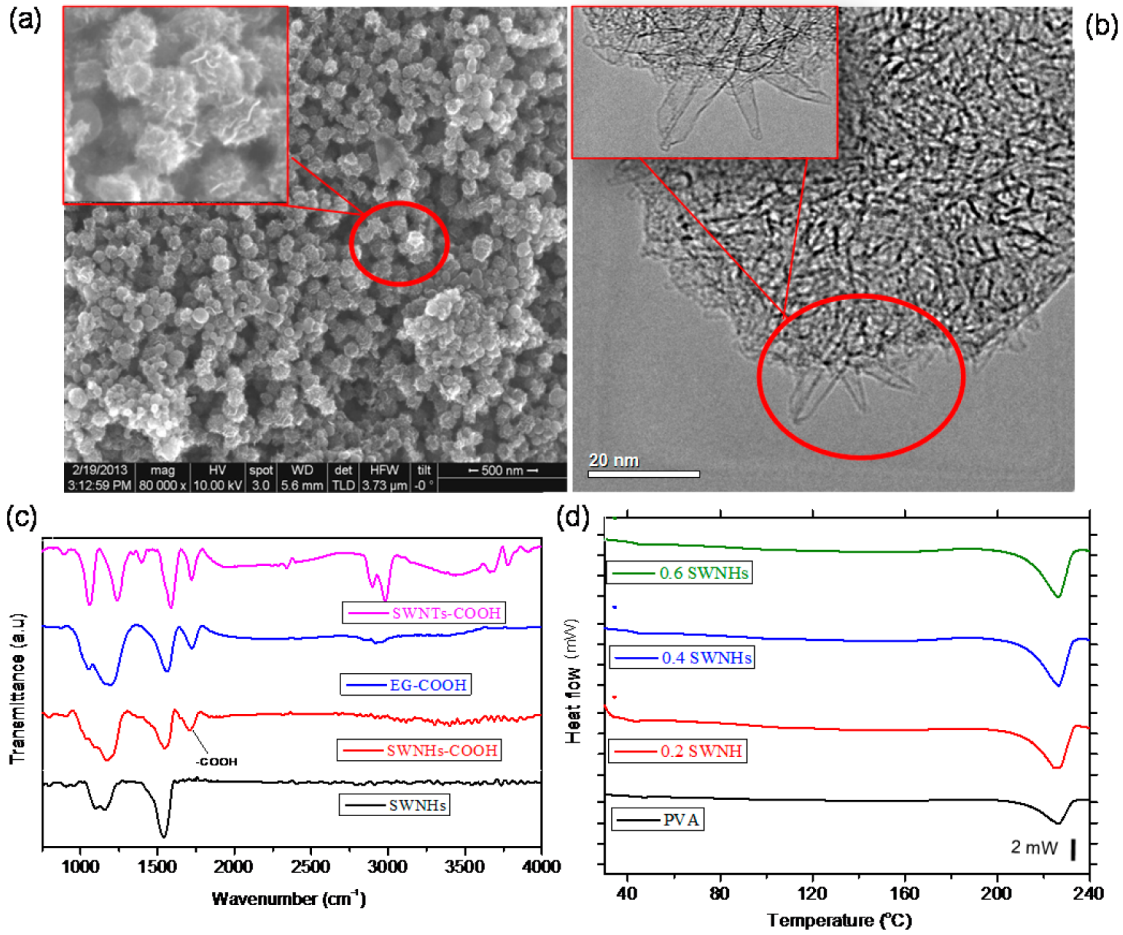

Figure 1. (a) FESEM and (b) TEM images of SWNHs. The inset in panel b shows the HRTEM image of dahlia-shaped aggregates, with the closed ends of SWNHs protruding outward. The results presented in panel b are part of a previous study by Pramoda et al.[11] on the synthesis and characterization of SWNHs, and are presented here for illustrative purposes. (c) The infrared spectra of pristine SWNHs and acid-functionalized SWNHs, SWNTs, and EG; the peak at 1720 cm^{-1} for the functionalized nanocarbons confirms the presence of carboxyl groups. (d) DSC scans of SWNH–PVA composites, showing endothermic peaks in the temperature range of 230–240 °C.

structural applications. In this regard, nanocarbon composites with polymer matrix material such as epoxy,[13] poly(methyl methacrylate),[14] polystyrene,[15] polyurethane,[16,17] poly(vinylidine fluoride),[18] Nafion,[19] and poly(ethylene terephthalate),[20] among others, have been studied and found suitable for applications requiring enhanced mechanical, thermal, or electrical properties.

Prasad et al.[4] have recently shown that the addition of more than one nanocarbon to a polymer matrix leads to extraordinary synergy in terms of the mechanical performance of the composite. This discovery, which opens a new paradigm for strengthening polymers, was subsequently validated for other functional properties, such as electrical conductivity. The rationale behind such a marked enhancement in properties comes from the fact that nanocarbons of different dimensionalities interact with the polymer chains in different ways and, when used together, provide synergistic benefits. In this regard, it would seem that SWNHs, which show one-dimensionality (single nanohorn protrusion) and three-dimensionality (spherical aggregate), in combination with a nanocarbon such as graphene, which is two-dimensional, could offer such benefits. Therefore, as a second objective of this study, we explore binary PVA composites reinforced by the combination of SWNHs and graphene.

2. EXPERIMENTAL SECTION

2.1. Synthesis and Characterization. SWNHs were prepared by DC-arc discharge of graphite rods in liquid nitrogen and were then functionalized by treating with a mixture of sulfuric acid and aqueous hydrogen peroxide (30%) at 80 °C for 2 h. The functionalized SWNHs were dispersed in distilled water by sonication. SWNH–PVA composites were then prepared as follows. First, a PVA solution was prepared by adding PVA to water at 60 °C while being subjected to continuous stirring. The dispersed SWNHs, with weight percentages of 0.2, 0.4 and 0.6, were added to this and sonicated for an additional 900 s. The obtained dispersion was dried in a Petri dish at 40–50 °C under vacuum over a period of 4–5 days and subsequently desiccated in $CaCl_2$ for 7 days to ensure complete removal of moisture from the composite. Pure PVA without nanocarbon addition and binary PVA composites with 0.4 wt % SWNH and 0.2, 0.4, and 0.6 wt % EG were prepared by following the aforementioned steps.

Graphene (EG) with 3–4 layers were obtained by thermal exfoliation of graphite oxide; the latter was prepared using the modified Hummer's method.[21] SWNTs with 98% purity were acquired from Comocat (Sigma–Aldrich). Both of them were functionalized by acid treatment using the following procedure: EG (50 mg) and SWNTs (50 mg) were separately taken in a solution of concentrated nitric acid (2 mL), sulfuric acid (2 mL), and distilled water (16 mL), and were heated in a microwave oven for 5–8 min under hydrothermal conditions to obtain a dispersed mixture. This mixture was then heated in an oven for 12 h at 100 °C and later filtered

DOI: 10.1021/acsami.5b02792
ACS Appl. Mater. Interfaces 2015, 7, 17016–17022

Table 1. Summary of Mechanical Properties and Degree of Crystallinity of Single Nanocarbon PVA Composite

nanofiller	elastic modulus, E (GPa)	hardness, H (MPa)	Viscosity Parameters from Maxwell–Voigt Fit		degree of crystallinity, χ (%)
			η_1 (GPa s)	η_2 (GPa s)	
none	0.27 ± 0.01	25.6 ± 1.23	241	4.5	38.1
0.2 wt % EG	0.36 ± 0.02	29.1 ± 2.07	278	4.6	41.8
0.4 wt % EG	0.76 ± 0.03	47.5 ± 1.14	172	7.4	41.9
0.6 wt % EG	0.69 ± 0.03	44.9 ± 3.80	301	5.3	42.4
0.2 wt % SWNH	0.80 ± 0.03	48.6 ± 0.99	165	6.7	42.0
0.4 wt % SWNH	1.12 ± 0.03	59.8 ± 1.84	160	9.0	44.4
0.6 wt % SWNH	0.98 ± 0.02	47.3 ± 1.72	171	6.1	44.8
0.2 wt % SWNT	1.21 ± 0.07	56.5 ± 2.80	586	12.3	46.3
0.4 wt % SWNT	1.80 ± 0.04	88.8 ± 2.40	356	28.6	46.3
0.6 wt % SWNT	2.94 ± 0.08	101.0 ± 4.50	760	48.9	48.0

through a sintered glass funnel by repeatedly washing with distilled water to ensure complete removal of acid. The obtained fuctionalized nanocarbons showed good dispersion in water, compared to their pristine form. EG–PVA and SWNT–PVA composites were obtained using the same procedure mentioned for SWNH–PVA.

Infrared (IR) spectroscopy was performed on the functionalized SWNHs to confirm the introduction of hydroxyl (−OH) and carboxyl ($-CO_2H$) groups. Differential scanning calorimetry (DSC) was performed on all of the composite samples (10 mg each) in a Mettler–Toledo system using a scan rate of 0.08 K/s in the temperature range of 40–250 °C. SWNHs were characterized by scanning electron microscopy (SEM) and transmission electron microscopy (TEM), following our previous study.[11]

2.2. Nanoindentation. All nanoindentation tests were carried out using a TriboIndenter system (Hysitron, Inc., Minneapolis, MN, USA). A minimum of 25 indentations each was performed on PVA and PVA–nanocomposite films using a peak load (P_{max}) of 500 μN and a loading rate of 0.5 mN/s. Penetration depths (<4 μm) corresponding to this load, despite being large, are significantly smaller than 5% of the film thickness (0.5 mm or more), thus ensuring the negligible effect of the substrate on measured properties.[22] To reduce/eliminate artifacts in E and H estimation, because of the viscoelastic behavior of PVA, the following procedure was utilized. A spheroconical tip (1 μm radius) was used to reduce large creep displacements produced by commonly used sharp tips;[23,24] the unload curves from these preliminary indentations and E and H obtained from them are shown in Figure S1 in the Supporting Information. A prolonged hold period of 250 s was found to be necessary to allow time for viscoelastic relaxation and, subsequently, to avoid the effect of creep on the unload curve, which otherwise results in an overestimation of E. A relatively high unload rate of 2 mN/s was used to minimize viscoelastic recovery and to obtain a convergent solution to the power-law fit (see the Supporting Information for detailed analysis). These load function parameters were also used for the composites as they showed a similar or a more dampened viscoelastic response.

E was extracted from the unloading curve by fitting it to a power-law relation given by Oliver and Pharr.[25] H was taken as the instantaneous value, obtained as P_{max} divided by the contact area at the end of loading. To ensure precise estimations, the tip area function was calibrated in a high depth range (0.5–4.5 μm) prior to testing. For this, optically clear polycarbonate (PC) with a modulus of 2.44 GPa was used. PC was preferred to the conventionally used fused quartz, since the latter does not facilitate large displacements required here, and has also been found unsuitable as a calibration standard for polymers for various reasons.[26]

3. RESULTS

Figures 1a and 1b show SEM and TEM micrographs, respectively, from which the aggregated, spherical morphology of SWNHs are seen. Some of these aggregates show outward protrusions of individual SWNHs. Figure 1c shows the IR spectra of pristine SWNHs and acid-functionalized SWNHs, SWNTs, and EG. After acid functionalization, the peak at 1720 cm^{-1} confirms the successful introduction of carboxyl ($-CO_2H$) groups. Figure 1d, as well as Figures S3a and S3b in the Supporting Information, show the DSC curves obtained for SWNH–PVA, SWNT–PVA, and EG–PVAcomposites, respectively. Note that the increase in area of the peak upon nanocarbon (especially SWNH) addition indicates an increase in the crystalline content of the reinforced PVA. Figure S4 in the Supporting Information shows typical N_2 adsorption–desorption isotherms for SWNTs and SWNHs. The surface areas of SWNTs and SWNHs were found to be 340 and 320 m^2/g, respectively.

The mechanical properties (elastic modulus (E), and hardness (H)) of PVA and its composites with SWNHs, SWNTs, and EG are presented in Table 1 and are plotted as functions of the filler concentration in Figure 2. From these, enhancements in E and H are observed upon addition of SWNHs to PVA, with a maximum occurring at 0.4 wt %; this amounts to an increase of ∼315% in E and ∼135% in H over the values for the unreinforced polymer. A decrease in E and H is observed with further increases in the SWNH concentration. In comparison, upon the addition of SWNTs, a maximum increment of ∼990% in E and ∼295% in H is observed at 0.6 wt %, whereas, with the addition of EG, a maximum improvement of ∼180% in E and ∼85% in H is observed at 0.4 wt %. The observed increment in E for the case of SWNT is consistent with that (∼1080%) reported by Eswar Prasad et al.[4] As a general observation, for a certain filler composition, SWNHs provide greater strengthening, compared to EG, and lesser strengthening, compared to SWNTs. However, note that the E and H values for 0.4SWNH–PVA and 0.2SWNT–PVA are similar.

Since 0.4 wt % addition is the most effective with SWNHs, this composition was considered as the base for examining its synergistic effect with EG. The results for these binary nanofiller composites are presented in Figure 3a and Table 2. Upon an addition of just 0.2 wt % of EG to 0.4 wt % SWNH, increases in E and H values, corresponding to increments of

DOI: 10.1021/acsami.5b02792
ACS Appl. Mater. Interfaces 2015, 7, 17016–17022

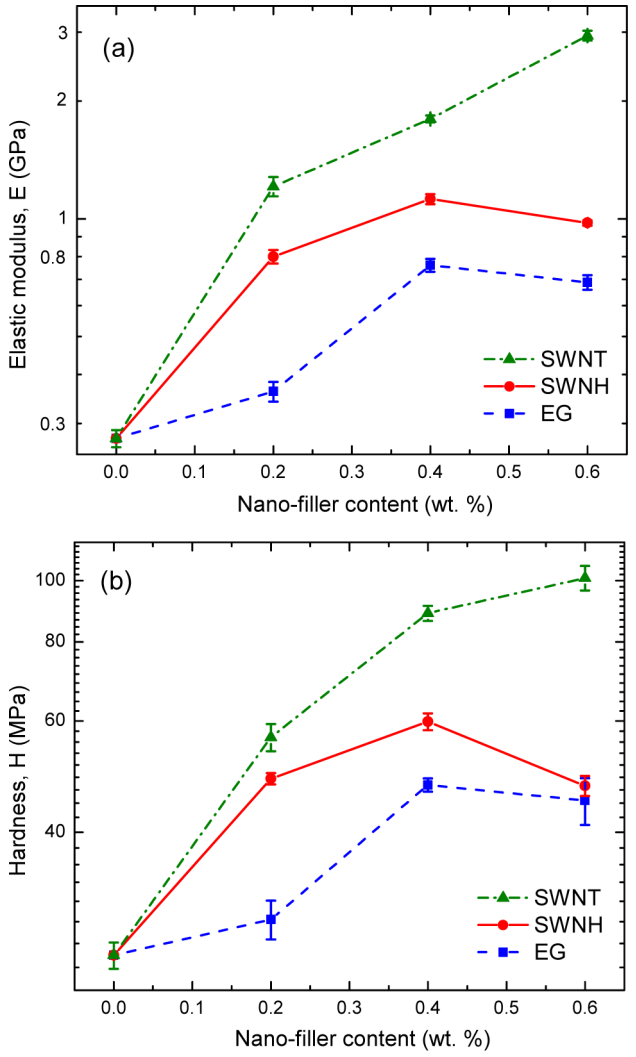

Figure 2. (a) Elastic modulus (E) of PVA and its nanocomposites for different nanocarbons and weight percentages, obtained from nanoindentation unloading response. (b) Variation of instantaneous hardness (H) for the same, calculated as the maximum applied load divided by the contact area at the end of loading. Note that the y-axis for both panels a and b are shown in logarithmic scale.

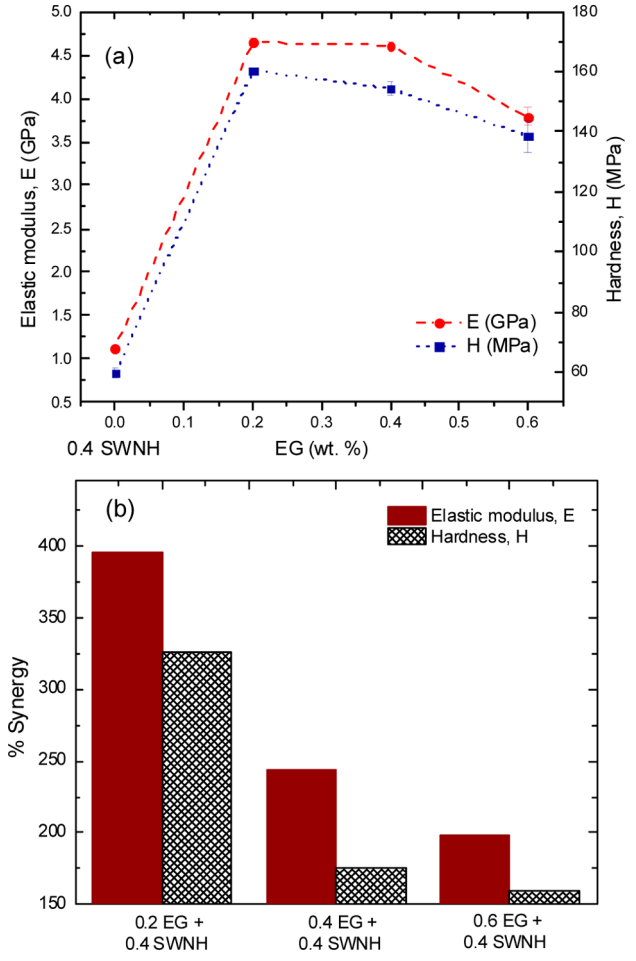

Figure 3. (a) Variation of elastic modulus (E) and hardness (H) for binary nanocomposites, with 0.2, 0.4, and 0.6 wt % EG in PVA added in combination with 0.4 wt % SWNH. (b) Synergy in E and H, upon binary addition of SWNH and EG, estimated using eq 1, with respect to the total mechanical property improvement upon individual nanocarbon additions. Average values of E and H were used for this calculation.

more than 4 and 2.5 times, respectively, is observed. With further additions, a slight decrease is noticed. However, the properties remain significantly higher than those of SWNH–PVA composites. The resulting synergistic effect is evaluated using the following expression and is presented in Figure 3b.

$$\text{synergy}\,(\%) = \frac{P_{\text{SWNH+EG}} - (\Delta P_{\text{SWNH}} + \Delta P_{\text{EG}})}{\Delta P_{\text{SWNH}} + \Delta P_{\text{EG}}} \times 100 \quad (1)$$

Here, $P_{\text{SWNH+EG}}$ is the average mechanical property (E or H) of the binary composite and ΔP is the change in average mechanical property upon the addition of a single nanofiller (either SWNH or EG) to PVA. The results show a maximum synergy of ~400% in E and ~330% in H.

The degree of crystallinity (χ) for PVA and its composites was calculated from DSC scans (see Figure 1d, as well as Figures S3a and S3b in the Supporting Information) as the ratio of the heat required to melt 1 g of dry sample (area of the peak between 230–240 °C) to that of the standard enthalpy of pure crystalline PVA ($\Delta H \approx 138.6$ J/g). The values obtained for single and binary nanocarbon composites are tabulated in Tables 1 and 2, respectively. The effectiveness of single nanocarbons in increasing χ is seen to rank in the following order: SWNT > SWNH > EG. The correspondence between the enhancement in E and the increase in χ are shown in Figure 4. A parabolic relation is seen to hold for the single nanocarbon composite, while the binary nanocarbon composite deviates from this trend. While the increase in χ for 0.4SWNH–0.2EG–PVA is just ~2% over that of 0.4SWNH–PVA, the increments in E and H for the same are ~315% and ~170%, respectively.

Next, to evaluate the effect of nanocarbon type and content on the polymer's viscous properties, a representative hold-time curve obtained from nanoindentation on PVA and its composites were empirically fit to a four-element Maxwell–Voigt model. The model, modified for the case of a conical indenter with a semicone angle, α, is given by Fischer-Cripps[23] as

$$h^2 = \left(\frac{\pi}{2}\right) P_0 \cot\alpha \left\{ \frac{1}{E_1} + \frac{1}{E_2}\left[1 - \exp\left(-\frac{tE_2}{\eta_2}\right)\right] + \left(\frac{1}{\eta_1}\right) t \right\} \quad (2)$$

DOI: 10.1021/acsami.5b02792
ACS Appl. Mater. Interfaces 2015, 7, 17016–17022

Table 2. Summary of Mechanical Properties and Degree of Crystallinity of Binary Nanocarbon PVA Composite

			Synergy (%)		Viscosity Parameters from Maxwell–Voigt Fit		
EG (wt %) + 0.4 NH	elastic modulus, E (GPa)	hardness, H (MPa)	elastic modulus	hardness	η_1 (GPa s)	η_2 (GPa s)	degree of crystallinity, χ (%)
0	1.12 ± 0.03	59.8 ± 1.84	0	0	160	9	44.4
0.2	4.65 ± 0.04	160.5 ± 0.89	395	326	4555	152	45.3
0.4	4.61 ± 0.03	154.4 ± 2.32	244	175	1990	149	45.2
0.6	3.79 ± 0.10	138.6 ± 5.30	198	159	906	97	45.7

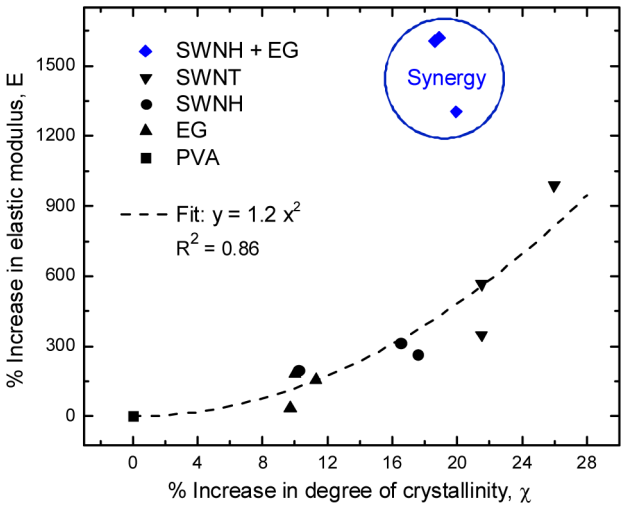

Figure 4. Increase in elastic modulus (E), with respect to increases in the degree of crystallinity (χ), for single and binary PVA composite. EG–PVA, SWNH–PVA, and SWNT–PVA composites show the dependence between the change in χ and change in E. The binary composite is seen to deviate from this trend.

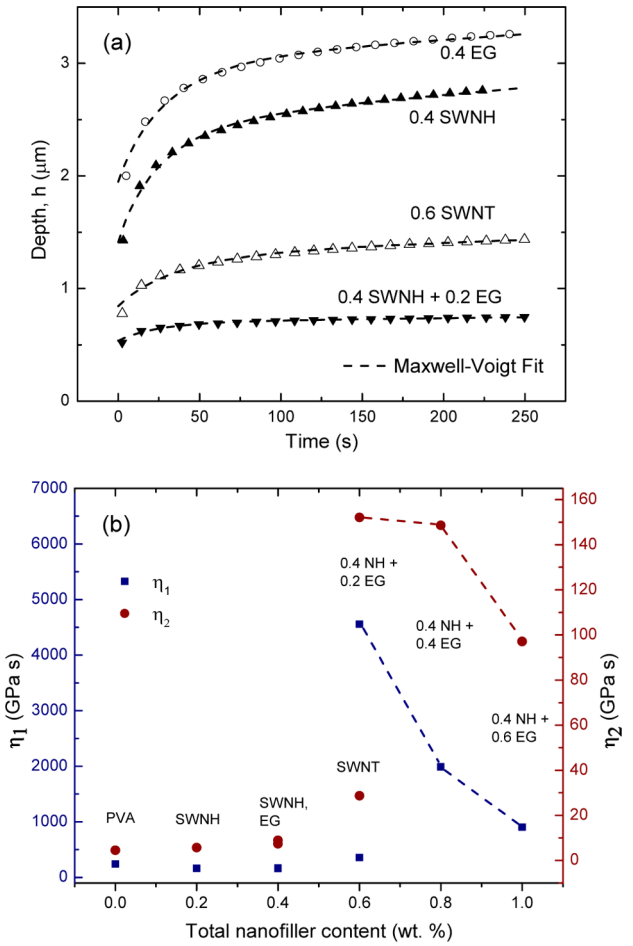

Figure 5. (a) Hold-time responses of some of the PVA nanocomposites are shown. The experimental creep curves are empirically fit to a four-element Maxwell–Voigt model (with a goodness of fit of $R^2 > 0.85$ for all). (b) The viscosity terms (η_1 and η_2) obtained from the fit shown in panel a are plotted against their filler composition. Note the high resistance to creep or hold-time deformation of the SWNH–EG–PVA composites.

Here, E_1 and E_2 are the spring constants representing the instantaneous and relaxation modulus, respectively, and η_1 and η_2 are the viscosity terms representing the time-dependent behavior. Since E has been obtained accurately from the Oliver–Pharr method, E_1 and E_2 obtained from the fit are of little importance and, hence, are not considered for discussion in this study. α was found to be 35° from the area function calibration on PC. The empirical fit to a few of the hold-time curves are shown in Figure 5a. Note that the fit does not fully reflect the experimental conditions as the model assumes a step load to P_{max} and, moreover, does not account for any plastic displacement.

Variations of η_1 and η_2, presented in Figure 5b, show minor changes upon EG and SWNH addition to PVA, while a noticeable increase is observed for the case of SWNT. Prior studies, investigating the effect of nanocarbons on the time-dependent deformation of polymers, have shown either a substantial or a minor reduction in creep response upon addition of graphene,[27,28] and a significant reduction upon addition of SWNTs,[29] both of which agree well with the present results. For the binary filler addition, EG plus SWNH, a substantial increment is seen, signifying a very high resistance to creep.

4. DISCUSSION

The substantial improvement in mechanical properties obtained through nanocarbon additions to polymer matrix is due to the fact that the functionalized nanocarbons containing $-CO_2H$ and $-OH$ groups (Figure 1c) act to bridge the weak van der Waals interaction between the polymer chains by forming stronger hydrogen bonds. In addition, the nanocarbons nucleate crystalline phases in the polymer as indicated by χ obtained from the DSC curves. In this context, the following factors hold the key in strengthening the polymer: the availability of a large surface area for interaction and the uniformity of nanocarbon dispersion.

For SWNH addition, experimental results (Figure 4) indicate that the enhancement in E and H are due, in part, to the formation of crystalline phases in PVA. Among the nanocarbons studied here, SWNTs are seen to induce the largest change in χ. This is attributed to its one-dimensionality and small size, which allows good interaction of the polymer chains and the nanotubes, inducing the nucleation of crystalline phases

DOI: 10.1021/acsami.5b02792
ACS Appl. Mater. Interfaces 2015, 7, 17016–17022

in the polymer.[1,4] For SWNHs, however, the fact that they occur as three-dimensional aggregates (as seen in Figures 1a and 1b) with aggregate diameters of 50−100 nm,[11] and not as individual, one-dimensional SWNHs, results in a relatively low interaction area, in comparison to SWNTs. Note here that individual SWNHs belong to the family of SWNTs and have a tube length and diameter of 10−70 nm and 2−10 nm, respectively.[30] While the measured BET surface areas are ∼340 m^2/g for SWNTs and ∼320 m^2/g for SWNHs, the surface area available for interaction with polymer chains will differ significantly from the measured values, which include the pore area present in the nanocarbons (see Figure S3 in the Supporting Information). For SWNTs, the dispersion from bundles during chemical functionalization and the use of water-soluble PVA for composite preparation enhances the interaction area. On the other hand, SWNH aggregates are not dispersed into individual nanohorns. Chemical functionalization and the use of water-soluble polymer only aids to separate one SWNH aggregate from another. Still, the reasonable change in χ (18%) induced by SWNH aggregates is probably due to the benefit of the interaction area provided by its spherical geometry, and also due to the outward protrusions of SWNH's conical ends (see "dahlia-shaped" aggregate in the inset in Figure 1b), which act in a one-dimensional manner akin to SWNTs. The reason for EG effecting a small change in χ is due to the limited locations at the edges of graphene sheet where functional groups can be induced[31] and also the multilayered nature (3−4 layers), which reduce the availability of the effective interfacial area.[32] Altogether, the effect of dimensionality on χ and on the mechanical properties is seen to increase as EG (2D), SWNHs (1D and 3D), and SWNTs (1D).

The experimental results presented in this work show that the combined addition of SWNHs and EG results in synergistic improvements (Figure 3) in E and H of the composites. It appears that the synergy, which is quite substantial, is mediated by a mechanism other than crystalline-phase nucleation (Figure 4). Also, the binary addition is observed to significantly suppress the hold-time creep (Figure 5). Quantitatively, this is reflected by the large increment in the viscosity parameters, η_1 and η_2, which signifies a transition from the fluidlike response of PVA (η_1 = 241 GPa s, η_2 = 4.5 GPa s) and the single nanofiller composites to a more solidlike response of the binary composite (η_1 = 4555 GPa s, η_2 = 152 GPa s). With no significant increase in χ, the enhanced resistance to viscoelastic creep is likely due to the hindered mobility of the molecular chains during deformation, which is possibly a result of the strong interaction of the fillers with the amorphous regions in the polymer. Interestingly, in a previous study,[4] the synergistic benefits obtained with the binary combinations of SWNT, EG, and ND were found to be independent of the crystallinity of the polymer and was attributed to an improved interaction between the nanocarbons and the polymer chains. With regard to practical applicability, the observation of an increase in the resistance to time-dependent deformation of PVA with SWNH and EG addition (Figure 5b) provides the possibility for designing polymer composites for applications where dimensional stability is of importance.

The reduction or constancy in the mechanical properties (except for SWNT−PVA) of the composites at high filler concentration (Figure 3) is due to the problem of agglomeration. Among SWNHs, there is likely to be local clustering of SWNH aggregates. This is confirmed by the increase in scatter in H values and $P-h$ responses (see Figure S2 in the Supporting Information), which is inferred to the increase in inhomogeneity within the composite film. Also, the concurrent decrease in η_1 and η_2 reflects the higher mobility of polymer chains, which signifies weakening of filler−matrix interaction as a consequence of agglomeration. Such agglomeration could not be detected by optical microscopy or through Raman spectra. The latter, which was collected at different locations of the composite (Figure S5 in the Supporting Information), showed peaks corresponding to both PVA and nanocarbon, signifying a generally good distribution of the nanocarbon. However, the local concentration of the nanocarbon could not be assessed, because of the high intensity of the obtained nanocarbon signal.

With PVA being of limited use in engineering and structural applications, the concern here is whether the results obtained in this study using PVA as the matrix material could translate to a similar performance in other polymers of practical importance. Since the mechanical property enhancement here is believed to be governed by the amount of crystalline phase and the nucleation of the same upon SWNH addition, this strengthening mechanism would seem applicable to other polymers that are semicrystalline in nature. In an earlier study, Cadek et al.[33] reasoned the greater increment in the mechanical properties of PVA—over an amorphous polymer—to the additional crystalline component formed upon carbon nanotube addition to the semicrystalline PVA matrix. Thus, the strengthening behavior of nanocarbon-reinforced polymers is likely to be dependent on the amorphous/crystalline nature of the polymer, the nature of SWNHs' functionalization, and the ease of SWNH dispersion within the polymer, with the latter two factors influencing the interaction potential.

While excellent improvements in E and H are observed upon SWNH addition and SWNH + EG binary addition, SWNHs occur in the form of spherically aggregated entities. As with SWNTs, in which well-dispersed individual nanotubes provide a larger surface area for interaction, compared to the cylindrically bundled nanotubes, individual SWNHs separated from spherical aggregates can be expected to substantially improve the surface area available for interaction, because of its one-dimensionality. The study by Zhang et al.,[30] which describes a process for such a separation of SWNH aggregates into individual entities, offers interesting possibilities for the further study of SWNH-reinforced polymer matrix composites.

5. CONCLUSIONS

The potential offered by SWNHs to strengthen a semicrystalline polymer (PVA) has been explored. Upon SWNH addition, substantial improvements in the elastic modulus and hardness are observed, the cause of which is the increase in the degree of crystallinity of the polymer. The properties obtained with SWNHs are better than those offered by the graphene EG, and at a certain composition comparable to those obtained with SWNTs. The combined addition of SWNH and EG to PVA results in extraordinary synergy in the mechanical properties and a high resistance to viscoelastic creep. Both of these are attributed (at low filler concentration) to a high degree of interaction between the filler and the matrix, but are found to be independent of the degree of crystallinity. The results of this study, in view of the commercial difficulty in producing SWNT composites, offer a new scope as SWNH composites can be produced economically. Further studies to determine properties such as ductility and toughness, and to understand the

DOI: 10.1021/acsami.5b02792
ACS Appl. Mater. Interfaces 2015, 7, 17016−17022

mechanism of synergistic improvements in mechanical properties, would be beneficial.

■ ASSOCIATED CONTENT

Supporting Information

Results of preliminary nanoindentation on PVA; detailed analysis to optimize load−function parameters used in this study; $P-h$ curves of 0.2EG−0.4SWNH−PVA and 0.6EG−0.4SWNH−PVA composites; DSC scans of SWNT−PVA and EG−PVA composites; nitrogen sorption profile and pore size distribution curves of SWNHs and SWNTs; Raman spectra of PVA, pristine SWNHs, and SWNH−PVA composites.The Supporting Information is available free of charge on the ACS Publications website at DOI: 10.1021/acsami.5b02792.

■ AUTHOR INFORMATION

Corresponding Author

*Tel.: +91 80 2293 3241. E-mail: ramu@materials.iisc.ernet.in.

Author Contributions

§All authors have given approval to the final version of the manuscript. These authors contributed equally to this work.

Notes

The authors declare no competing financial interest.

■ REFERENCES

(1) Coleman, J. N.; Khan, U.; Blau, W. J.; Gun'ko, Y. K. Small but Strong: A Review of the Mechanical Properties of Carbon Nanotube−Polymer Composites. *Carbon* **2006**, *44*, 1624−1652.

(2) Ramanathan, T.; Abdala, A. A.; Stankovich, S.; Dikin, D. A.; Herrera-Alonso, M.; Piner, R. D.; Adamson, D. H.; Schniepp, H. C.; Chen, X.; Ruoff, R. S.; Nguyen, S. T.; Aksay, I. A.; Prud'Homme, R. K.; Brinson, L. C. Functionalized Graphene Sheets for Polymer Nanocomposites. *Nat. Nanotechnol.* **2008**, *3*, 327−331.

(3) Maitra, U.; Prasad, K. E.; Ramamurty, U.; Rao, C. N. R. Mechanical Properties of Nanodiamond-Reinforced Polymer−Matrix Composites. *Solid State Commun.* **2009**, *149*, 1693−1697.

(4) Prasad, K. E.; Das, B.; Maitra, U.; Ramamurty, U.; Rao, C. N. R. Extraordinary Synergy in the Mechanical Properties of Polymer Matrix Composites Reinforced with 2 Nanocarbons. *Proc. Natl. Acad. Sci. U. S. A.* **2009**, *106*, 13186−13189.

(5) Ajayan, P. M.; Zhou, O. Z. *Applications of Carbon Nanotubes*; Dresselhaus, M. S., Dresselhaus, G., Avouris, P., Eds.; Topics in Applied Physics, Vol. *80*; Springer: Berlin, Heidelberg, 2001; pp 391−425.

(6) Liu, Y.; Kumar, S. Polymer/carbon Nanotube Nano Composite Fibers—A Review. *ACS Appl. Mater. Interfaces* **2014**, *6*, 6069−6087.

(7) Harris, P. J. F. Carbon Nanotube Composites. *Int. Mater. Rev.* **2004**, *49*, 31−43.

(8) Vivekchand, S. R. C.; Jayakanth, R.; Govindaraj, A.; Rao, C. N. R. The Problem of Purifying Single-Walled Carbon Nanotubes. *Small* **2005**, *1*, 920−923.

(9) Azami, T.; Kasuya, D.; Yuge, R.; Yudasaka, M.; Iijima, S.; Yoshitake, T.; Kubo, Y. Large-Scale Production of Single-Wall Carbon Nanohorns with High Purity. *J. Phys. Chem. C* **2008**, *112*, 1330−1334.

(10) Iijima, S.; Yudasaka, M.; Yamada, R.; Bandow, S.; Suenaga, K.; Kokai, F.; Takahashi, K. Nano-Aggregates of Single-Walled Graphitic Carbon Nano-Horns. *Chem. Phys. Lett.* **1999**, *309*, 165−170.

(11) Pramoda, K.; Moses, K.; Ikram, M.; Vasu, K.; Govindaraj, A.; Rao, C. N. R. Synthesis, Characterization and Properties of Single-Walled Carbon Nanohorns. *J. Cluster Sci.* **2014**, *25*, 173−188.

(12) Cioffi, C.; Campidelli, S.; Sooambar, C.; Marcaccio, M.; Marcolongo, G.; Meneghetti, M.; Paolucci, D.; Paolucci, F.; Ehli, C.; Rahman, G. M. A.; Sgobba, V.; Guldi, D. M.; Prato, P. Synthesis, Characterization, and Photoinduced Electron Transfer in Functionalized Single Wall Carbon Nanohorns. *J. Am. Chem. Soc.* **2007**, *129*, 3938−3945.

(13) Ajayan, P. M.; Schadler, L. S.; Giannaris, C.; Rubio, A. Single-Walled Carbon Nanotube−Polymer Composites: Strength and Weakness. *Adv. Mater.* **2000**, *12*, 750−753.

(14) Das, B.; Eswar Prasad, K.; Ramamurty, U.; Rao, C. N. R. Nano-Indentation Studies on Polymer Matrix Composites Reinforced by Few-Layer Graphene. *Nanotechnology* **2009**, *20*, 125705.

(15) Qian, D.; Dickey, E. C.; Andrews, R.; Rantell, T. Load Transfer and Deformation Mechanisms in Carbon Nanotube-Polystyrene Composites. *Appl. Phys. Lett.* **2000**, *76*, 2868.

(16) Gupta, T. K.; Singh, B. P.; Tripathi, R. K.; Dhakate, S. R.; Singh, V. N.; Panwar, O. S.; Mathur, R. B. Superior Nano-Mechanical Properties of Reduced Graphene Oxide Reinforced Polyurethane Composites. *RSC Adv.* **2015**, *5*, 16921−16930.

(17) Wang, X.; Hu, Y.; Song, L.; Yang, H.; Xing, W.; Lu, H. *In Situ* Polymerization of Graphene Nanosheets and Polyurethane with Enhanced Mechanical and Thermal Properties. *J. Mater. Chem.* **2011**, *21*, 4222.

(18) Ansari, S.; Giannelis, E. P. Functionalized Graphene Sheet−Poly(vinylidene Fluoride) Conductive Nanocomposites. *J. Polym. Sci., Part B: Polym. Phys.* **2009**, *47*, 888−897.

(19) Lee, S.; Choi, B. G.; Choi, D.; Park, H. S. Nanoindentation of Annealed Nafion/sulfonated Graphene Oxide Nanocomposite Membranes for the Measurement of Mechanical Properties. *J. Membr. Sci.* **2014**, *451*, 40−45.

(20) Li, M.; Jeong, Y. G. Poly(ethylene Terephthalate)/exfoliated Graphite Nanocomposites with Improved Thermal Stability, Mechanical and Electrical Properties. *Composites, Part A* **2011**, *42*, 560−566.

(21) Hummers, W. S.; Offeman, R. E. Preparation of Graphitic Oxide. *J. Am. Chem. Soc.* **1958**, *80*, 1339.

(22) Ramamurty, U.; Jang, J. Nanoindentation for Probing the Mechanical Behavior of Molecular Crystals−A Review of the Technique and How to Use It. *CrystEngComm* **2014**, *16*, 12−23.

(23) Fischer-Cripps, A. C. A Simple Phenomenological Approach to Nanoindentation Creep. *Mater. Sci. Eng., A* **2004**, *385*, 74−82.

(24) Klapperich, C.; Komvopoulos, K.; Pruitt, L. Nanomechanical Properties of Polymers Determined from Nanoindentation Experiments. *J. Tribol.* **2001**, *123*, 624.

(25) Oliver, W. C.; Pharr, G. M. An Improved Technique for Determining Hardness and Elastic Modulus Using Load and Displacement Sensing Indentation Experiments. *J. Mater. Res.* **1992**, *7*, 1564−1583.

(26) Briscoe, B. J.; Fiori, L.; Pelillo, E. Nano-Indentation of Polymeric Surfaces. *J. Phys. D: Appl. Phys.* **1998**, *31*, 2395−2405.

(27) Chen, J.; Guo, X.; Tang, Q.; Zhuang, C.; Liu, J.; Wu, S.; Beake, B. D. Nanomechanical Properties of Graphene on Poly(ethylene Terephthalate) Substrate. *Carbon* **2013**, *55*, 144−150.

(28) King, J. A.; Klimek, D. R.; Miskioglu, I.; Odegard, G. M. Mechanical Properties of Graphene Nanoplatelet/epoxy Composites. *J. Appl. Polym. Sci.* **2013**, *128*, 4217−4223.

(29) Tehrani, M.; Safdari, M.; Al-Haik, M. S. Nanocharacterization of Creep Behavior of Multiwall Carbon Nanotubes/Epoxy Nanocomposite. *Int. J. Plast.* **2011**, *27*, 887−901.

(30) Zhang, M.; Yamaguchi, T.; Iijima, S.; Yudasaka, M. Individual Single-Wall Carbon Nanohorns Separated from Aggregates. *J. Phys. Chem. C* **2009**, *113*, 11184−11186.

(31) Cheng, H. K. F.; Sahoo, N. G.; Tan, Y. P.; Pan, Y.; Bao, H.; Li, L.; Chan, S. H.; Zhao, J. Poly(vinyl Alcohol) Nanocomposites Filled with Poly(vinyl Alcohol)-Grafted Graphene Oxide. *ACS Appl. Mater. Interfaces* **2012**, *4*, 2387−2394.

(32) Kiran, M. S. R. N.; Raidongia, K.; Ramamurty, U.; Rao, C. N. R. Improved Mechanical Properties of Polymer Nanocomposites Incorporating Graphene-like BN: Dependence on the Number of BN Layers. *Scr. Mater.* **2011**, *64*, 592−595.

(33) Cadek, M.; Coleman, J. N.; Barron, V.; Hedicke, K.; Blau, W. J. Morphological and Mechanical Properties of Carbon-Nanotube-Reinforced Semicrystalline and Amorphous Polymer Composites. *Appl. Phys. Lett.* **2002**, *81*, 5123.

DOI: 10.1021/acsami.5b02792
ACS Appl. Mater. Interfaces 2015, 7, 17016−17022